Research Article

Angiotensin-(1–7) reduces α-synuclein aggregation by enhancing autophagic activity in Parkinson's disease

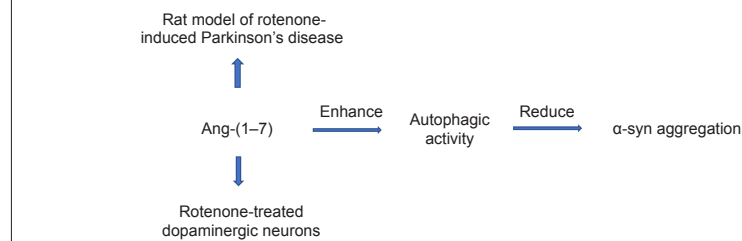Qing Gao, Rui Chen, Liang Wu, Qing Huang, Xi-Xi Wang, You-Yong Tian[*], Ying-Dong Zhang[*]

Graphical Abstract *Angiotensin-(1–7) has potential therapeutic value for Parkinson's disease*

Abstract

Abnormal accumulation of α-synuclein contributes to the formation of Lewy bodies in the substantia nigra, which is considered the typical pathological hallmark of Parkinson's disease. Recent research indicates that angiotensin-(1–7) plays a crucial role in several neurodegenerative disorders, including Parkinson's disease, but the underlying mechanisms remain elusive. In this study, we used intraperitoneal administration of rotenone to male Sprague-Dawley rats for 4 weeks to establish a Parkinson's disease model. We investigated whether angiotensin-(1–7) is neuroprotective in this model by continuous administration of angiotensin-(1–7) into the right substantia nigra for 4 weeks. We found that angiotensin-(1–7) infusion relieved characteristic parkinsonian behaviors and reduced α-synuclein aggregation in the substantia nigra. Primary dopaminergic neurons were extracted from newborn Sprague-Dawley rat substantia nigras and treated with rotenone, angiotensin-(1–7), and/or the Mas receptor blocker A-779 for 24 hours. After binding to the Mas receptor, angiotensin-(1–7) attenuated apoptosis and α-synuclein aggregation in rotenone-treated cells. Primary dopaminergic neurons were also treated with angiotensin-(1–7) and/or the autophagy inhibitor 3-methyladenine for 24 hours. Angiotensin-(1–7) increased α-synuclein removal and increased the autophagy of rotenone-treated cells. We conclude that angiotensin-(1–7) reduces α-synuclein aggregation by alleviating autophagy dysfunction in Parkinson's disease. Therefore, the angiotensin-(1–7)/Mas receptor axis plays an important role in the pathogenesis of Parkinson's disease and angiotensin-(1–7) has potential therapeutic value for Parkinson's disease. All experiments were approved by the Biological Research Ethics Committee of Nanjing First Hospital (approval No. DWSY-2000932) in January 2020.

Key Words: α-synuclein; apoptosis; autophagy; dopaminergic neuron; Lewy bodies; neurodegenerative diseases; Parkinson's disease; renin-angiotensin system; rotenone; substantia nigra

Chinese Library Classification No. R459.9; R363; R364

Introduction

The renin-angiotensin system (RAS) plays a crucial role in regulating blood pressure and water and sodium homeostasis in the circulation (Perez-Lloret et al., 2017; Janatpour and Symes, 2020). Increasing evidence indicates that the brain has a local RAS independent of peripheral organs. Angiotensin II (Ang II) and Ang II type 1 receptor (AT1R) constitute a classic pathway of the RAS in the brain and are involved in Parkinson's disease (PD) and other neurological diseases (Gao et al., 2016). Angiotensin-(1–7) [Ang-(1–7)] is a recently discovered bioactive peptide of RAS that is of increasing interest to researchers. Ang-(1–7) and its Mas receptor (MasR) bypass RAS, which antagonizes several physiological impacts of the Ang II/AT1R axis and may play a protective role in many neurodegenerative disorders, including PD (Kehoe et al., 2016; Rabie et al., 2018). However, the mechanisms by which Ang-(1–7) participates in PD are still elusive.

PD is the second-most-prevalent neurodegenerative disease (Ascherio and Schwarzschild, 2016). Loss of dopaminergic cells and the formation of Lewy bodies (LBs) in the substantia nigra (SN) are typical pathological markers of PD (Gao et al., 2016). Recently, as the main component of LBs, α-synuclein (α-syn) has attracted increasing attention. Abnormal aggregation of α-syn results in the onset of LB formation and is linked to the progression of PD and other α-synucleinopathies (Flagmeier et al., 2016; Chiti and Dobson, 2017; Shahnawaz et al., 2020), but the specific mechanisms are not completely understood.

As a conserved cellular process, autophagy involves the segregation of cell organelles and proteins into autophagosomes, followed by degradation in the lysosomes and reuse of macromolecules (Scrivo et al., 2018). Properly regulated autophagy eliminates impaired organelles and aggregate-prone proteins, thus maintaining cellular homeostasis. Therefore, autophagy has been regarded as the

Department of Neurology, Nanjing First Hospital, Nanjing Medical University, Nanjing, Jiangsu Province, China
*Correspondence to: Ying-Dong Zhang, MD, PhD, zhangyingdong@aliyun.com; You-Yong Tian, PhD, tyy9956@163.com.
https://orcid.org/0000-0002-6470-5064 (Ying-Dong Zhang); https://orcid.org/0000-0001-9338-4346 (You-Yong Tian)

main means of clearance of abnormally accumulated α-syn (Xilouri et al., 2016; Choi et al., 2020). Autophagic dysfunction and α-syn pathology exist in PD patients and in animal models of PD (Fan et al., 2019; Bellomo et al., 2020; Zou et al., 2020). On consideration of the above evidence, impaired clearance of α-syn caused by defective autophagic activity may be a pivotal contributing factor in the onset of PD.

Therefore, we speculated that Ang-(1–7) attenuates α-syn pathology by alleviating autophagic dysfunction in PD. In this study, we used the rotenone-induced PD rat model to investigate the effects of Ang-(1–7) on parkinsonian behaviors and α-syn pathology. Meanwhile, we explored the influence of Ang-(1–7)/MasR on α-syn aggregation and autophagic activity in a rotenone-induced PD cell model.

Materials and Methods

Animals and treatments
Sixty-eight male Sprague-Dawley (SD) rats, aged 7 weeks and weighing 250–280 g, were acquired from the Animal Core Facility of Nanjing Medical University (license No. SCXK (Zhe) 2019-0001). The rats were raised in an air-conditioned space under a 12-hour diurnal cycle and provided sufficient water and food. The animal experiments were conducted at Nanjing First Hospital under the Guide for the Care and Use of Laboratory Animals. All experiments were approved by the Biological Research Ethics Committee of Nanjing First Hospital in January 2020 (approval number: DWSY-2000932).

To determine whether the Ang-(1–7)/MasR axis was altered during PD progression, a PD rat model was generated, as previously described (Javed et al., 2016; Jayaraj et al., 2020). Briefly, rats received intraperitoneal injection of rotenone daily for 4 weeks to establish the model. Rotenone (MilliporeSigma, St. Louis, MO, USA) was dissolved in dimethyl sulfoxide and then added to sunflower oil to achieve a concentration of 2.5 mg/mL. We randomly divided 17 rats into two groups. The control group (n = 7) received intraperitoneal administration of vehicle only, and the PD group (n = 10) received intraperitoneal administration of prepared rotenone (2.5 mg/kg) once a day for 4 weeks. The rat models of PD were successfully established according to catalepsy tests, in which PD models have significantly prolonged descent latency compared with control rats. To investigate whether exogenous infusion of Ang-(1–7) (MilliporeSigma) exerted neuroprotection in PD rats, Ang-(1–7) was continuously injected into the right SN for 4 weeks, in conjunction with the rotenone treatment described above. We randomly divided 51 rats into three groups. Group 1 rats (control, n = 12) received supranigral infusion of artificial cerebrospinal fluid (aCSF) (0.25 μL/hour) and intraperitoneal administration of vehicle, group 2 rats (PD, n = 20) received supranigral infusion of aCSF (0.25 μL/hour) and intraperitoneal administration of rotenone (2.5 mg/kg), and group 3 rats (PD + Ang-(1–7), n = 19) received supranigral infusion of Ang-(1–7) (1.1 nmol/0.25 μL/hour) and intraperitoneal administration of rotenone (2.5 mg/kg). The dose of Ang-(1–7) was chosen in accordance with our previous report (Jiang et al., 2013).

Supranigral infusion
The right-side supranigral infusion was administered using an osmotic pump (model 2004, ALZET, Cupertino, CA, USA) connected to a cannula, as previously described (Wang et al., 2018a). Pumps were primed with 37°C sterile saline for 40 hours before implantation. After inhalation anesthesia with isoflurane (Abbott Laboratories, Shanghai, China) in medical O₂ (5% for induction, 2% for maintenance) (Van Den Berge et al., 2019), rats were positioned in a stereotactic frame (David Kopf Instruments, Tujunga, CA, USA). The stainless-steel infusion cannula was placed at preset coordinates of the right

supranigral region (anteroposterior, –5.2 mm; mediolateral, –2.1 mm; dorsoventral, –7.8 mm from bregma) (Bok et al., 2018). Pumps were implanted subcutaneously on the backs of the rats. The supranigral infusion was continuously performed for 4 weeks in conjunction with the rotenone treatment.

Catalepsy tests
We assessed catalepsy using a grid test and a bar test (Tong et al., 2016). Tests were carried out after 4 weeks of injection of rotenone, Ang-(1–7), or vehicle, as described (Tong et al., 2016). In the grid test, a gridiron with 1-cm spaces between wires was used. We measured the time from when all paws of the rat were hung on the grid until it took one paw from the grid (Tong et al., 2016). The time taken was defined as the descent latency. In the bar test, each rat was hung by its forepaws on a metal rod. The time taken before the rat fell from the bar was defined as the descent latency. The maximum time was set at 120 seconds. Each rat had three trials for each test. The mean value of the three trials for each rat was calculated and analyzed.

Blood pressure assessments
Systolic blood pressure (SBP) was assessed by tail cuff (Visitech Systems, Apex, NC, USA) weekly in the afternoon from baseline (10 weeks old) until the end of treatment (14 weeks old), as described (Park et al., 2020). Each assessment was conducted three times to achieve a mean SBP.

Evaluation of Ang-(1–7) levels in the substantia nigra
To assess Ang-(1–7) levels, SN sections were separated and homogenized after the 4-week administration of vehicle or rotenone, then centrifuged at 1000 × g and 4°C for 15 minutes to remove cellular debris. The supernatant was stored at –80°C until use. The Ang-(1–7) levels in the SN were detected by enzyme-linked immunosorbent assay (S-1330, BMA Biomedicals, Augst, Switzerland), as previously described (Tao et al., 2018).

Immunohistochemical staining
Immunohistochemical staining was carried out as previously described (Wang et al., 2018b). In brief, after the 4-week supranigral infusion, the rat brains were dissected in 4% paraformaldehyde. Coronal sections (from 24.5 mm to 26.2 mm caudal to the bregma) were cut into 5-μm-thick sections using a sliding microtome. The SN-containing sections were dewaxed, hydrated, and submerged in 0.3% H₂O₂ for 0.5 hours. Subsequently, samples were treated with 0.5% Triton X-100 for 0.5 hours, blocked for approximately 0.5 hours with 5% bovine serum albumin, and incubated overnight at 4°C with a rabbit monoclonal antibody against α-syn (1:200, Cat# 4179, RRID: AB_1904156; Cell Signaling Technology Inc., Beverly, MA, USA). The slides were treated at 37°C for 1 hour with biotinylated anti-rabbit IgG (Immunostain SP Kit, PV-9000; OriGene Technologies, Rockville, MD, USA). Next, slides were stained with diaminobenzidine and counterstained with hematoxylin. Finally, the sections were dehydrated, cover slipped, and scanned under a fluorescent microscope (Olympus Corporation, Tokyo, Japan). We counted cells in five randomly selected non-overlapping fields for each slide. Data from the five fields were added together, and that total was expressed as a percentage of the total number of cells in the relevant fields.

Cell culture and experimental groups
Primary rat midbrain dopaminergic neurons were prepared according to a previous study (Peng et al., 2018). Briefly, the midbrain was quickly dissected from the ventral mesencephalon of gestational day 14 SD rat embryos (Daehan Biolink, Daejeon, South Korea). Tissues were digested with

Research Article

0.25% trypsin in Hanks' balanced salt solution at 37°C for 10 minutes, filtered, and centrifuged for 5 minutes. The isolated neurons were transferred to Dulbecco's modified Eagle medium with 10% fetal bovine serum and incubated in a poly-L-lysine-coated plate at 37°C with 5% CO_2 for 4 hours. The medium was then changed to Neurobasal medium containing 2% B27. The maturation to midbrain dopaminergic neurons took 8 days. The medium was replaced every 2 days.

To investigate the influence of Ang-(1–7) on the rotenone-induced cell model, the neurons were randomly divided into four groups. For the control group (n = 3), primary dopaminergic neurons were cultured with Neurobasal medium containing 2% B27; for the rotenone (ROT) group (n = 3), neurons were cultured with rotenone (100 nM) for 24 hours; for the ROT + Ang-(1–7) group (n = 3), neurons were co-cultured with rotenone (100 nM) and Ang-(1–7) (100 nM) for 24 hours; and for the ROT + Ang-(1–7) + A-779 (a MasR blocker, Abbiotec Inc., Escondido, CA, USA) group (n = 3), neurons were co-cultured with rotenone (100 nM), Ang-(1–7) (100 nM), and A-779 (1 µM) for 24 hours.

To investigate the relationship between autophagy and α-syn aggregation, the cells were divided into another four groups. For the control group (n = 3), primary dopaminergic neurons were cultured with Neurobasal medium containing 2% B27; for the ROT group (n = 3), neurons were cultured with rotenone (100 nM) for 24 hours; for the ROT + Ang-(1–7) group (n = 3), neurons were co-cultured with rotenone (100 nM) and Ang-(1–7) (100 nM) for 24 hours; and for the ROT + Ang-(1–7) + 3-methyladenine (3-MA, an autophagy blocker; MilliporeSigma) group (n = 3), neurons were co-cultured with rotenone (100 nM), Ang-(1–7) (100 nM), and 3-MA (5 mM) for 24 hours. The doses of rotenone, Ang-(1–7), A-779, and 3-MA were selected according to previous studies (Gao et al., 2016; Liu et al., 2018; Zhou et al., 2018).

Western blot assay

Western blot assay samples were prepared and analyzed according to a previous study (Jiang et al., 2016). The same amount of protein from different groups was resolved by 10–15% sodium dodecyl sulfate-polyacrylamide gels, transferred to polyvinylidene fluoride membranes, and blocked for 60 minutes in 5% nonfat milk. All membranes were incubated overnight at 4°C in primary antibody: rabbit polyclonal antibody against Mas receptor (1:2000, NBP1-78444, RRID: AB_11039164; Novus Biologicals, Centennial, CO, USA), rabbit monoclonal antibody against α-syn (1:1000, Cat# 4179, RRID: AB_1904156; Cell Signaling Technology Inc.), rabbit polyclonal antibody against cleaved caspase-3 (1:1000, Cat# 9661, RRID: AB_2341188; Cell Signaling Technology Inc.), rabbit monoclonal antibody against p62 (1:10,000, ab109012, RRID: AB_2810880; Abcam, Cambridge, MA, USA), rabbit polyclonal antibody against microtubule associated protein 1 light chain 3 (LC3) (1:1000, Cat# 2775, RRID: AB_915950; Cell Signaling Technology Inc.), or rabbit monoclonal antibody against β-actin (1:200, Cat# BM3873, Wuhan Boster Biological Technology Ltd., Wuhan, China). After rinsing in 1× Tris-buffered saline with 0.1% Tween 20, membranes were incubated with horseradish peroxidase-coupled anti-rabbit secondary antibody (1:3000, Cat# 7074, RRID:AB_2099233; Cell Signaling Technology Inc.) for 2 hours at room temperature. Finally, after washing with 1× Tris-buffered saline with 0.1% Tween 20, protein bands were detected for 5 minutes by using a chemiluminescent horseradish peroxidase substrate (Thermo Fisher Scientific, Waltham, MA, USA) and an automated chemiluminescence imaging system (Tanon Science & Technology, Shanghai, China). The gray value of protein bands was assessed using ImageJ 1.44 software (NIH, Bethesda, MD, USA) and was normalized to β-actin.

Colorimetric assay of caspase-3 activity

After the indicated treatment for 24 hours, neurons were lysed in extraction buffer (Beyotime Biotechnology, Shanghai, China), as previously described (Gao et al., 2016). The caspase-3 activity was quantified using a fluorometric assay kit (ab252897, Abcam), in accordance with the manufacturer's instructions.

Immunofluorescence analysis

Immunofluorescence analysis was conducted as previously described (Gao et al., 2016). After receiving 24-hour drug treatment, neurons were collected, fixed in 4% paraformaldehyde for 10 minutes, and permeabilized in 0.5% Triton X-100. After washing in PBS and blocking for 10 minutes, cells were incubated overnight at 4°C with primary antibodies: a rabbit polyclonal antibody against lysosomal-associated membrane protein 2A (LAMP2A, 1:200, Cat# 51-2200, RRID: AB_2533900; Thermo Fisher Scientific) and a mouse monoclonal antibody against α-syn (1:200, Cat# MA5-12272, RRID: AB_10978319; Thermo Fisher Scientific). The neurons were rinsed in PBS, cultured with anti-rabbit Alexa Fluor 488–conjugated secondary antibody (green) (1:200, ab150077, RRID: AB_2630356; Abcam) and anti-mouse Alexa Fluor 594–conjugated secondary antibody (red) (1:200, ab150116, RRID: AB_2650601; Abcam) in the dark for 1 hour at 37°C. The nuclei were counterstained with 4',6-diamidino-2-phenylindole (DAPI) (Vector Laboratories Inc., Burlingame, CA, USA) and observed by fluorescent microscopy (Olympus Corporation). Fluorescence intensity was measured by ImageJ software (NIH) and normalized to fluorescence intensity of the control group.

Statistical analysis

All statistical analyses were conducted using Prism 6 software (GraphPad, San Diego, CA, USA). Data were calculated as the mean ± SD. Statistical comparisons between groups were performed using Student's t-test, one-way analysis of variance with Tukey's *post hoc* test, and two-way repeated measures analysis of variance with Bonferroni's multiple comparisons test. A level of $P < 0.05$ was considered statistically significant.

Results

Effects of rotenone infusion on systolic blood pressure of Sprague-Dawley rats

As indicated in **Figure 1A** and **B**, PD rat models were established after 4-week treatment with rotenone and were confirmed by prolonged descent latency in comparison with control rats ($P < 0.0001$). No significant changes in SBP of rats were observed throughout the study ($P > 0.05$; **Figure 1C**).

Ang-(1–7)/MasR axis is reduced in the substantia nigra of the PD rat model

A time point analysis was performed to investigate whether Ang-(1–7) and MasR are related to the pathogenesis of PD. As demonstrated by **Figure 2A**, the Ang-(1–7) level in the SN of 14-week-old PD rats was significantly lower than that in age-matched control rats ($P < 0.0001$). As shown in **Figure 2B** and C, Western blot assay revealed a noticeable decrease in MasR levels in the SN of 14-week-old PD rats compared with age-matched control rats ($P < 0.0001$). These findings show that the Ang-(1–7)/MasR axis may be involved in PD.

Exogenous Ang-(1–7) infusion relieves characteristic parkinsonian behaviors and reduces the aggregation of α-synuclein in the substantia nigra in the rotenone-induced PD rat model

To verify the pharmacological influence of Ang-(1–7) and

to investigate its potential for translation into a clinical application, rats were continuously injected with vehicle or exogenous Ang-(1–7) for 4 weeks together with rotenone infusion. During the study, there was no significant change in SBP ($P > 0.05$; **Figure 3A**). Catalepsy tests were conducted to investigate whether exogenous Ang-(1–7) infusion can alleviate the characteristic parkinsonian behaviors of PD rats. The grid test and bar test both revealed that the descent latency in the PD group was significantly reduced following Ang-(1–7) treatment ($P < 0.0001$ and $P < 0.001$, respectively; **Figure 3B** and **C**). Afterwards, as indicated in **Figure 3D** and **E**, the increased aggregation of α-syn in the SN of PD rats was reduced following Ang-(1–7) treatment ($P < 0.0001$). This result was also demonstrated by Western blot with an anti-α-syn antibody (**Figure 3F** and **G**). In summary, Ang-(1–7) rescued characteristic PD symptoms and reduced α-syn aggregation in the SN of PD rats.

Ang-(1–7) attenuates apoptosis in the rotenone-induced cell model in a MasR-dependent manner

In this study, primary dopaminergic neurons extracted from ventral mesencephalon were cultured with rotenone for 24 hours. To further investigate the connection between the Ang-(1–7)/MasR axis and PD pathogenesis, the neurons were cultured with Ang-(1–7) and the MasR antagonist A-779 for 24 hours concurrently. We detected cleaved caspase-3 expression to investigate the influence of the Ang-(1–7)/MasR axis on apoptosis. As indicated in **Figure 4A** and **B**, rotenone increased the level of cleaved caspase-3 by approximately fivefold ($P < 0.001$). However, the increased level of cleaved caspase-3 was completely reversed by Ang-(1–7) ($P < 0.01$). Furthermore, co-treatment with A-779 significantly abolished this influence caused by Ang-(1–7) ($P < 0.05$), which indicates the process is MasR-dependent manner. This result was further demonstrated by assessment of the caspase-3 activity (**Figure 4C**). These observations reveal that Ang-(1–7) rescues apoptosis in the rotenone-induced cell model in a MasR-dependent manner.

Ang-(1–7) attenuates α-synuclein accumulation in the rotenone-induced cell model in a MasR-dependent manner

To investigate the influence of the Ang-(1–7)/MasR axis on the pathology of PD, we detected α-syn expression. As seen in **Figure 5A** and **B**, rotenone-induced pathological changes were reversed by Ang-(1–7), as increased α-syn in the ROT group was markedly downregulated when incubated with Ang-(1–7) ($P < 0.01$). However, the influence caused by Ang-(1–7) was reversed when co-cultured with A-779, as the level of α-syn was distinctly higher than that of the group treated with Ang-(1–7) ($P < 0.05$). This finding was also demonstrated by immunofluorescence using an anti-α-syn antibody (**Figure 5C** and **D**). These results imply that Ang-(1–7) attenuates α-syn accumulation in the rotenone-induced cell model in a MasR-dependent manner.

Activation of autophagy contributes to the clearance of α-synuclein accumulation in the rotenone-induced cell model

First, we detected the expression of p62 and LC3-II to investigate whether Ang-(1–7) caused activation of autophagy in the rotenone-induced cell model. As revealed by **Figure 6A–C**, the rotenone-induced cell model had significantly increased p62 ($P < 0.001$) and significantly decreased LC3-II ($P < 0.0001$). However, after treatment with Ang-(1–7) together with rotenone, the defective autophagic activity in the ROT group was increased, as shown by **Figure 6B** ($P < 0.01$) and **Figure 6C** ($P < 0.001$). To determine the causal

relationship between α-syn clearance and autophagy, the cell model was co-incubated with Ang-(1–7) and 3-MA for 24 hours. As demonstrated by **Figure 6A–C**, the reduction of p62 levels induced by Ang-(1–7) was fully abolished by 3-MA ($P < 0.05$; **Figure 6B**), and the increase in LC3-II levels induced by Ang-(1–7) was also fully abolished by 3-MA ($P < 0.001$; **Figure 6C**), proving the suppressive influence of 3-MA in autophagy activation caused by Ang-(1–7). Notably, suppression of autophagy completely converted Ang-(1–7)-induced α-syn clearance in the cell model, as the decrease in α-syn level caused by Ang-(1–7) was also dramatically reversed by 3-MA ($P < 0.05$; **Figure 6D** and **E**). This finding was also demonstrated by immunofluorescence analysis with an antibody immunoreactive to the lysosomal-associated membrane protein 2A (LAMP2A, an indicator of chaperone-mediated autophagy) and an anti-α-syn antibody (**Figure 6F–H**). Taken together, these findings show that autophagic dysfunction exists in the rotenone-induced cell model, and activation of autophagy contributes to the clearance of α-syn.

Discussion

The RAS is an important circulating-hormone system, modulating blood pressure and maintaining water and sodium homeostasis. Mounting evidence indicates that many tissues and organs, including the central nervous system, have their own localized RAS. The Ang II/AT1R axis is a classic axis of the RAS and is implicated in numerous neurodegenerative disorders. Interestingly, bypass of the RAS is receiving ever more attention. Ang-(1–7), a recently discovered bioactive peptide of RAS, and the Mas receptor constitute the Ang-(1–7)/MasR axis, which regulates several physiological functions of the Ang II/AT1R axis. Recently, Costa-Besada et al. (2018) found that the Ang-(1–7)/MasR axis exists in dopaminergic neurons and resists the pro-oxidative activities of the Ang II/AT1R axis, which has been shown to aggravate neurodegeneration in PD models. Meanwhile, findings from Rabie's laboratory show that, by binding to the MasR, Ang-(1–7) confers neuroprotection against neurotoxicity induced by the Ang II/AT1R axis in a PD model (Rabie et al., 2018). Therefore, the Ang-(1–7)/MasR axis is potentially associated with PD progression. Consistent with these results, we show that Ang-(1–7) and MasR levels in the SN of 14-week-old PD rats are lower than those of age-matched controls, similar to results from clinical trials that detected lower plasma Ang-(1–7) levels in PD patients than in control individuals (Rocha et al., 2016). All these findings support the conclusion that the Ang-(1–7)/MasR axis has a protective impact during progression of PD.

To further investigate the relationship between Ang-(1–7) and PD pathogenesis, we infused exogenous Ang-(1–7) into the SN of PD rat models and control rats. We found that Ang-(1–7) infusion not only lessened typical behaviors in the rotenone-induced PD rat model but also reduced the aggregation of α-syn in the SN. Similarly, previous studies have found that Ang-(1–7) is associated with the etiology of several neurodegenerative disorders, such as Alzheimer's disease and hypertension-induced neurodegeneration, and plays a beneficial role in these disorders (Jiang et al., 2016; Ho and Nation, 2018; Cao et al., 2019). In line with this, the current study shows for the first time that Ang-(1–7) is also implicated in the pathogenesis of PD and, therefore, its use may be translated into a clinical application. Our findings not only emphasize the beneficial effect of the brain Ang-(1–7)/MasR axis in neurological disorders but also throw light on the potential of Ang-(1–7) for treating PD.
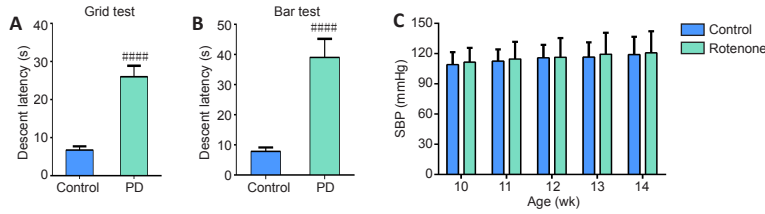
Figure 1 │ Effects of rotenone infusion on systolic blood pressure of Sprague-Dawley rats.
Rats were infused intraperitoneally with rotenone (2.5 mg/kg) or vehicle daily for 4 weeks. (A, B) Descent latency of control and PD rats in catalepsy tests was recorded. Data are the mean ± SD (*n* = 6; Student's *t*-test). ####*P* < 0.0001, *vs.* control group. (C) The SBP of rats was tracked by means of tail cuff, and differences were observed in the same group at different time points. Data are mean ± SD (*n* = 6; two-way repeated measures analysis of variance). No obvious changes in SBP of rats were seen in each group during the study *(P* > 0.05). 1 mmHg = 0.133 kPa. PD: Parkinson's disease; SBP: systolic blood pressure.
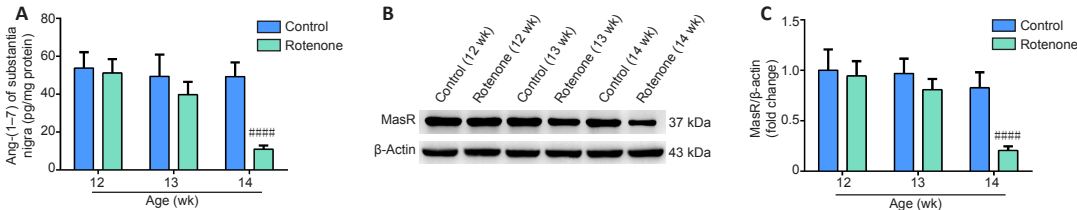
Figure 2 │ Ang-(1–7)/MasR axis is reduced in the substantia nigra of the Parkinson's disease rat model.
(A) The Ang-(1–7) levels in the SN were assessed by enzyme-linked immunosorbent assay. Differences were observed between PD rats and age-matched control rats. (B) The MasR levels in the SN were evaluated by Western blot assay. (C) Quantitative results of MasR expression. Differences were observed between PD rats and age-matched control rats. Data are expressed as the mean ± SD (*n* = 6; one-way analysis of variance followed by Tukey's *post hoc* test). ####*P* < 0.0001, *vs.* control group. PD: Parkinson's disease; MasR: Mas receptor; SN: substantia nigra; w: weeks.
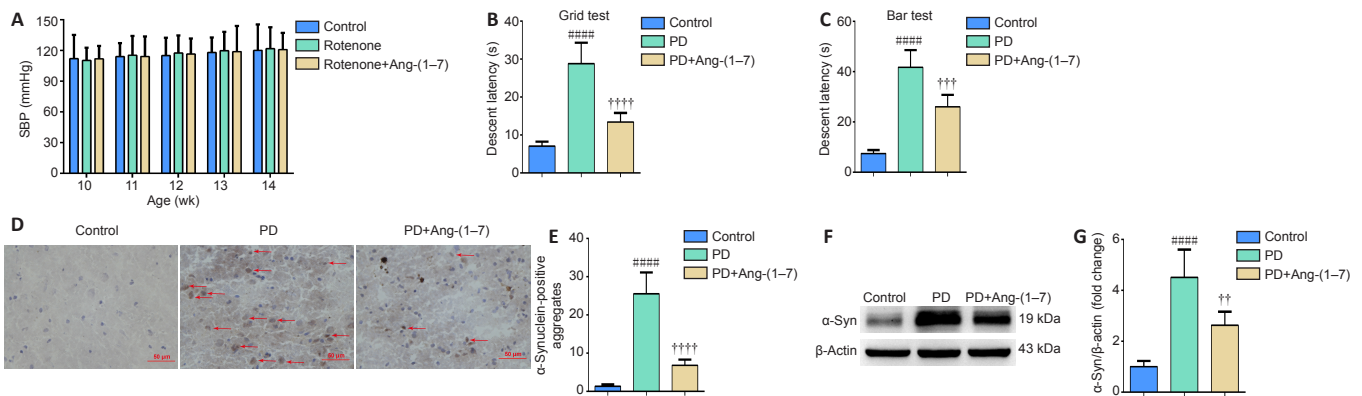

Figure 3 │ Exogenous Ang-(1–7) infusion relieves characteristic parkinsonian behaviors and reduces the aggregation of α-synuclein in the substantia nigra in the rotenone-induced Parkinson's disease rat model.
(A) The SBP of rats was tracked by means of tail cuff, and differences were observed in the same group for different time points. Data are expressioned as mean ± SD (*n* = 6; two-way repeated measures analysis of variance). There was no significant difference in the SBP of rats between groups during the study (*P* > 0.05). (B) Descent latency of different groups in catalepsy tests was determined by agrid test. (C) Descent latency of different groups was determined by bar test. (D) The α-syn pathology in the SN of different groups was observed by immunohistochemical staining and fluorescent microscopy (original magnification, 400×). After incubation with primary and secondary antibodies, slides were stained with diaminobenzidine and counterstained with hematoxylin. The red arrows indicate α-syn-positive aggregates. (E) Quantitative results of α-syn-positive aggregates. (F) The α-syn expression in the SN in different groups was detected by Western blot assay. (G) Quantitative results of α-syn expression. Data are expressioned as the mean ± SD (B, C, E, G: *n* = 6, one-way analysis of variance followed by Tukey's *post hoc* test). ####*P* < 0.0001, *vs.* control group; ††*P* < 0.01, †††*P* < 0.001, ††††*P* < 0.0001, *vs.* PD group. 1 mmHg = 0.133 kPa. Ang-(1–7): Angiotensin-(1–7); PD: Parkinson's disease; SBP: systolic blood pressure; SN: substantia nigra; w: weeks; α-syn: α-synuclein.
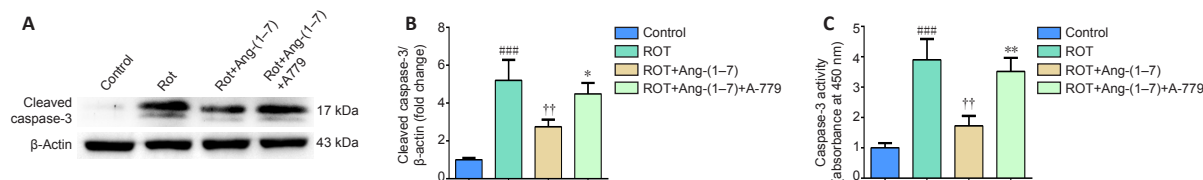

Figure 4 │ Ang-(1–7) attenuates apoptosis in the rotenone-induced cell model in a MasR-dependent manner.
(A) The cleaved caspase-3 levels of four groups were determined by Western blot assay. (B) Quantitative results of cleaved caspase-3 expression. (C) Caspase-3 activity was determined by colorimetric assay. Data are expressed as the mean ± SD (B, C: *n* = 3, one-way analysis of variance followed by Tukey's *post hoc* test). *P* < 0.05, **P* < 0.01, *vs.* ROT + Ang-(1–7) group; ###*P* < 0.001, *vs.* control group; ††*P* < 0.01, *vs.* ROT group. Ang-(1–7): Angiotensin-(1–7); MasR: Mas receptor; ROT: rotenone.

Figure 5 | Ang-(1–7) attenuates α-synuclein accumulation in the rotenone-induced cell model in a MasR-dependent manner.
(A) The expression of α-syn in four groups was examined by Western blot assay. (B) Quantitative results of α-syn expression. (C) Cells were marked by an anti-α-syn antibody (red), nuclei were counterstained with DAPI (blue), and immunofluorescence was observed by fluorescent microscopy (original magnification, 630×). Expression of α-syn was higher in the ROT group and was downregulated when incubated with Ang-(1–7). However, the influence caused by Ang-(1–7) was completely abolished with A-779 co-treatment. (D) Mean α-syn fluorescence intensity (ratio to control) of four groups. Data are expressed as the mean the ± SD (*n* = 3; one-way analysis of variance followed by Tukey's *post hoc* test). #*P* < 0.05, ##*P* < 0.01, *vs*. control group; †*P* < 0.05, ††*P* < 0.01, *vs*. ROT group; **P < 0.05, **P < 0.01, *vs*. ROT + Ang-(1–7) group. Ang-(1–7): Angiotensin-(1–7); DAPI: 4′,6-diamidino-2-phenylindole; MasR: Mas receptor; ROT: rotenone; α-syn: α-synuclein.
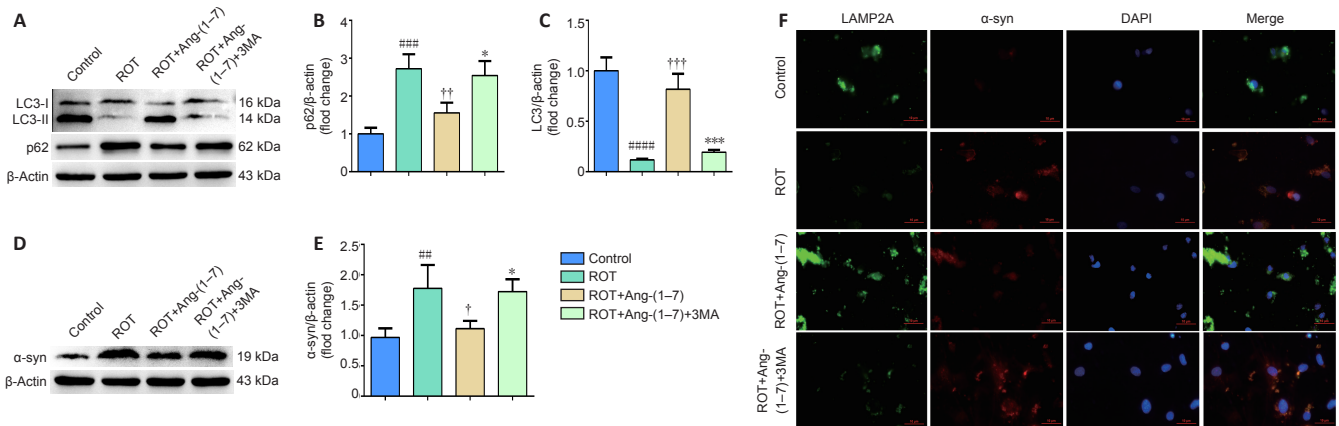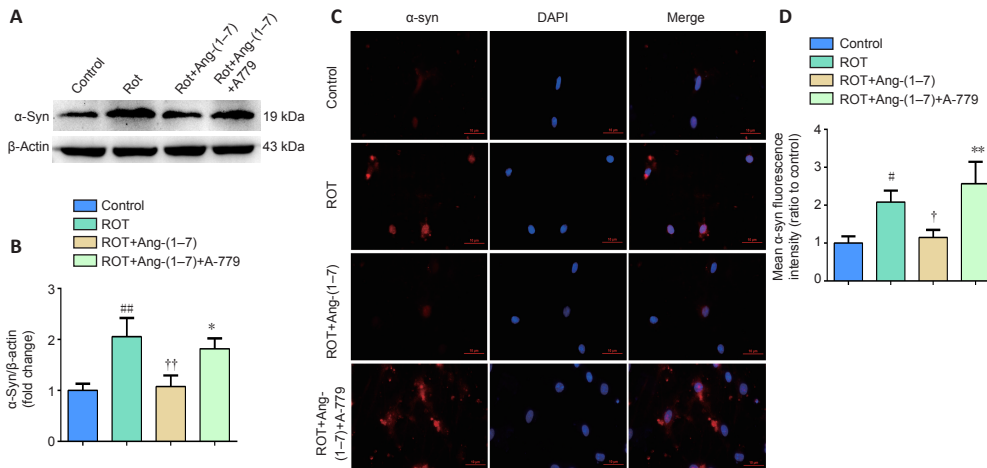

Figure 6 | Activation of autophagy contributes to the clearance of α-synuclein accumulation in the rotenone-induced cell model.
(A) The p62 and LC3-II levels were determined by Western blot assay. (B) Quantitative results of p62 expression. (C) Quantitative results of LC3-II expression. (D) The expression of α-syn was detected by Western blot assay. (E) Quantitative results of α-syn expression. (F) The number of LAMP2A-positive cells (green) and α-syn-positive cells (red) by immunofluorescence were observed with a fluorescent microscope (original magnification, 630×). (G) Mean LAMP2A fluorescent intensity (ratio to control) of four groups. (H) Mean α-syn fluorescence intensity (ratio to control) of four groups. Data are expressed as the mean ± SD (B, C, E; *n* = 3; one-way analysis of variance followed by Tukey's *post hoc* test). ##*P* < 0.01, ###*P* < 0.001, ####*P* < 0.0001, *vs*. control group; †*P* < 0.05, ††*P* < 0.01, †††*P* < 0.001, ††††*P* < 0.0001, vs. ROT group; **P < 0.05, ***P < 0.001, ****P < 0.0001, *vs*. ROT + Ang-(1–7) group. 3-MA: 3-Methyladenine; Ang-(1–7): angiotensin-(1–7); DAPI: 4′,6-diamidino-2-phenylindole; LAMP2A: lysosomal-associated membrane protein 2A; LC3: microtubule associated protein 1 light chain 3; ROT: rotenone; α-syn: α-synuclein.

To clarify how the Ang-(1–7)/MasR axis affects PD evolution, we established a cell model using rotenone incubation for 24 hours and determined apoptosis levels and α-syn expression in different groups. We found that Ang-(1–7) rescues the apoptosis of dopaminergic cells in the rotenone-treated group, as cleaved caspase-3 was remarkably decreased after Ang-(1–7) treatment. However, the impact of Ang-(1–7) was reversed when co-treated with A-779, an antagonist of the Mas receptor. This was further verified by a colorimetric assay for caspase-3 activity, which showed corresponding changes in different groups. These findings were consistent with a previous study showing that Ang-(1–7) can attenuate neuronal apoptosis in brains of hypertensive rats (Jiang et al., 2013). Meanwhile, by Western blot and immunofluorescence, we revealed that dramatically elevated α-syn levels in the

rotenone-induced cell model were lowered by Ang-(1–7) treatment. This effect was also significantly reduced by co-incubation with A-779. Our findings further strengthen the importance of the Ang-(1–7)/MasR axis in neurological diseases determined by previous studies (Costa-Besada et al., 2018; Rabie et al., 2018). To our knowledge, this study is the first to clarify that the Ang-(1–7)/MasR axis reduces apoptosis and α-syn pathology of dopaminergic neurons in a rotenone-induced cell model.

The underlying mechanisms by which the Ang-(1–7)/MasR axis reduces α-syn pathology in dopaminergic neurons are not completely discovered. There is evidence that autophagy plays a pivotal role in maintaining proper quantity and quality of protein and organelles in cells, and autophagic dysfunction

can lead to impaired α-syn degradation and abnormal α-syn aggregation (Xilouri et al., 2016). A recent study indicates that dysfunctional autophagy exists in PD models and in PD patients, which contributes to the pathogenesis of PD (Scrivo et al., 2018). In the present study, we verified the assumption that Ang-(1–7) reduces α-syn accumulation by reversing the dysfunctional autophagic activity in the rotenone-induced cell model. Western blot assay revealed that the level of LC3-II was decreased and the level of p62 was elevated in rotenone-treated neurons, indicating the existence of autophagic deficiency in the rotenone-induced cell model. However, Ang-(1–7) distinctly increased the autophagic activity, and the changes in LC3-II and p62 levels were inverted in the neurons co-treated with rotenone and Ang-(1–7). To date, our study is the first to show that Ang-(1–7) enhances autophagy in dopaminergic neurons. Our findings are supported by previous studies indicating that Ang-(1–7) improves autophagic activities in cells from other tissues (Lin et al., 2018; Pan et al., 2018). Proper autophagic activity removes accumulation-prone proteins and impaired organelles, while defective autophagy prevents the elimination of abnormally accumulated proteins and contributes to several neurodegenerative disorders (Xilouri et al., 2016). Similarly, our current study found that when the increased autophagic activity caused by Ang-(1–7) was antagonized by 3-MA, the level of α-syn was restored. This was further confirmed by immunofluorescence analysis, thus providing evidence that dysfunctional autophagy contributes to the α-syn pathology in a rotenone-induced PD cell model. Notably, unlimited autophagic activities may induce apoptosis of cells and result in numerous disorders. As indicated by our previous studies, Ang II induced unrestrained autophagy and led to apoptosis in a dopaminergic neuronal cell line called CATH.a, which was considered a contributing factor in the progression of PD (Gao et al., 2016). Therefore, autophagy is a double-edged sword in physiology and pathology, and autophagic intensity maybe depend on the inducer or cell type. Taken together, these findings uncover the mechanisms by which Ang-(1–7) reduces α-syn pathology in a rotenone-induced cell model and underline the damage from deficient autophagic activity in PD.

In this study, we prove for the first time that Ang-(1–7) improves autophagic dysfunction, thus contributing to the elimination of α-syn in PD models. This may reveal the potential mechanisms by which the Ang-(1–7)/MasR axis participates in PD.

Study limitations

There are limitations to our study. First, the rotenone model of PD has several disadvantages. The high systemic toxicity of rotenone may lead to a high mortality rate of rats. In addition, some treated rats do not display neurodegeneration due to rotenone resistance (Chia et al., 2020). Therefore, we used a sufficient number of rats to ensure the successful establishment of a PD model. Second, several studies have observed that α-syn can propagate in a prion-like manner in animal models by injection of preformed fibrils, which contributes to the pathological formation of PD (Jan et al., 2018; Elfarrash et al., 2019; Van Den Berge et al., 2019). In our current rotenone-induced PD rat model, we were not able to investigate the spreading manner of α-syn. In the future, we may investigate other mechanisms relevant to α-syn in PD. Third, there is extensive evidence showing that some phytochemicals confer neuroprotection in PD by counteracting the aggregation, toxicity, and prion-like spreading of α-syn through activation of autophagy (Limanaqi et al., 2019; Stacchiotti and Corsetti, 2020). Therefore, we can explore the potential role of Ang-(1–7) in α-syn toxicity and spreading in our future studies. Our research may reveal the potential

mechanisms by which Ang-(1–7)/MasR participates in PD and may strengthen the evidence for application of Ang-(1–7) as therapy for PD.

Conclusion

Our current study shows that the Ang-(1–7)/MasR axis reduces α-syn pathology in a rotenone-induced cell model by reducing dysfunctional autophagic activity. More importantly, our results imply potential of Ang-(1–7) for PD therapy *in vivo*. These findings deepen our insight into the protective mechanisms of the Ang-(1–7)/MasR axis during PD progression and support the development of related therapeutic strategies for the treatment of PD and other α-synucleinopathies.

References

Ascherio A, Schwarzschild MA (2016) The epidemiology of Parkinson's disease: risk factors and prevention. Lancet Neurol 15:1257-1272.

Bellomo G, Paciotti S, Gatticchi L, Parnetti L (2020) The vicious cycle between α-synuclein aggregation and autophagic-lysosomal dysfunction. Mov Disord 35:34-44.

Bok E, Chung YC, Kim KS, Baik HH, Shin WH, Jin BK (2018) Modulation of M1/M2 polarization by capsaicin contributes to the survival of dopaminergic neurons in the lipopolysaccharide-lesioned substantia nigra in vivo. Exp Mol Med 50:1-14.

Cao C, Hasegawa Y, Hayashi K, Takemoto Y, Kim-Mitsuyama S (2019) Chronic angiotensin 1-7 infusion prevents angiotensin-ii-induced cognitive dysfunction and skeletal muscle injury in a mouse model of Alzheimer's disease. J Alzheimers Dis 69:297-309.

Chia SJ, Tan EK, Chao YX (2020) Historical perspective: models of Parkinson's disease. Int J Mol Sci 21:2464.

Chiti F, Dobson CM (2017) Protein misfolding, amyloid formation, and human disease: a summary of progress over the last decade. Annu Rev Biochem 86:27-68.

Choi I, Zhang Y, Seegobin SP, Pruvost M, Wang Q, Purtell K, Zhang B, Yue Z (2020) Microglia clear neuron-released α-synuclein via selective autophagy and prevent neurodegeneration. Nat Commun 11:1386.

Costa-Besada MA, Valenzuela R, Garrido-Gil P, Villar-Cheda B, Parga JA, Lanciego JL, Labandeira-Garcia JL (2018) Paracrine and intracrine angiotensin 1-7/Mas receptor axis in the substantia Nigra of rodents, monkeys, and humans. Mol Neurobiol 55:5847-5867.

Elfarrash S, Jensen NM, Ferreira N, Betzer C, Thevathasan JV, Diekmann R, Adel M, Omar NM, Boraie MZ, Gad S, Ries J, Kirik D, Nabavi S, Jensen PH (2019) Organotypic slice culture model demonstrates inter-neuronal spreading of alpha-synuclein aggregates. Acta Neuropathol Commun 7:213.

Fan RZ, Guo M, Luo S, Cui M, Tieu K (2019) Exosome release and neuropathology induced by α-synuclein: new insights into protective mechanisms of Drp1 inhibition. Acta Neuropathol Commun 7:184.

Flagmeier P, Meisl G, Vendruscolo M, Knowles TP, Dobson CM, Buell AK, Galvagnion C (2016) Mutations associated with familial Parkinson's disease alter the initiation and amplification steps of α-synuclein aggregation. Proc Natl Acad Sci U S A 113:10328-10333.

Gao Q, Jiang T, Zhao HR, Wu L, Tian YY, Ou Z, Zhang L, Pan Y, Lu J, Zhang YD (2016) Activation of autophagy contributes to the angiotensin II-triggered apoptosis in a dopaminergic neuronal cell line. Mol Neurobiol 53:2911-2919.

Ho JK, Nation DA (2018) Cognitive benefits of angiotensin IV and angiotensin-(1-7): a systematic review of experimental studies. Neurosci Biobehav Rev 92:209-225.

Jan A, Jansonius B, Delaidelli A, Bhanshali F, An YA, Ferreira N, Smits LM, Negri GL, Schwamborn JC, Jensen PH, Mackenzie IR, Taubert S, Sorensen PH (2018) Activity of translation regulator eukaryotic elongation factor-2 kinase is increased in Parkinson disease brain and its inhibition reduces alpha synuclein toxicity. Acta Neuropathol Commun 6:54.

Janatpour ZC, Symes AJ (2020) The extended renin-angiotensin system: a promising target for traumatic brain injury therapeutics. Neural Regen Res 15:1025-1026.

Javed H, Azimullah S, Haque ME, Ojha SK (2016) Cannabinoid Type 2 (CB2) Receptors activation protects against oxidative stress and neuroinflammation associated dopaminergic neurodegeneration in rotenone model of Parkinson's disease. Front Neurosci 10:321.

Jayaraj RL, Beiram R, Azimullah S, Mf NM, Ojha SK, Adem A, Jalal FY (2020) Valeric acid protects dopaminergic neurons by suppressing oxidative stress, neuroinflammation and modulating autophagy pathways. Int J Mol Sci 21:7670.

Jiang T, Gao L, Shi JQ, Lu J, Wang Y, Zhang YD (2013) Angiotensin-(1-7) modulates renin-angiotensin system associated with reducing oxidative stress and attenuating neuronal apoptosis in the brain of hypertensive rats. Pharmacol Res 67:84-93.

Jiang T, Zhang YD, Zhou JS, Zhu XC, Tian YY, Zhao HD, Lu H, Gao Q, Tan L, Yu JT (2016) Angiotensin-(1-7) is reduced and inversely correlates with Tau hyperphosphorylation in animal models of Alzheimer's disease. Mol Neurobiol 53:2489-2497.

Kehoe PG, Wong S, Mulhim NL, Palmer LE, Miners JS (2016) Angiotensin-converting enzyme 2 is reduced in Alzheimer's disease in association with increasing amyloid-β and tau pathology. Alzheimers Res Ther 8:50.

Limanaqi F, Biagioni F, Busceti CL, Ryskalin L, Polzella M, Frati A, Fornai F (2019) Phytochemicals bridging autophagy induction and alpha-synuclein degradation in Parkinsonism. Int J Mol Sci 20:3274.

Lin YT, Wang HC, Chuang HC, Hsu YC, Yang MY, Chien CY (2018) Pre-treatment with angiotensin-(1-7) inhibits tumor growth via autophagy by downregulating PI3K/Akt/mTOR signaling in human nasopharyngeal carcinoma xenografts. J Mol Med (Berl) 96:1407-1418.

Liu J, Liu W, Lu Y, Tian H, Duan C, Lu L, Gao G, Wu X, Wang X, Yang H (2018) Piperlongumine restores the balance of autophagy and apoptosis by increasing BCL2 phosphorylation in rotenone-induced Parkinson disease models. Autophagy 14:845-861.

Pan M, Zheng Z, Chen Y, Sun N, Zheng B, Yang Q, Zhang Y, Li X, Meng Y (2018) Angiotensin-(1-7) attenuated cigarette smoking-related pulmonary fibrosis via improving the impaired autophagy caused by nicotinamide adenine dinucleotide phosphate reduced oxidase 4-dependent reactive oxygen species. Am J Respir Cell Mol Biol 59:306-319.

Park SH, Farooq MA, Gaertner S, Bruckert C, Qureshi AW, Lee HH, Benrahla D, Pollet B, Stephan D, Ohlmann P, Lessinger JM, Mayoux E, Auger C, Morel O, Schini-Kerth VB (2020) Empagliflozin improved systolic blood pressure, endothelial dysfunction and heart remodeling in the metabolic syndrome ZSF1 rat. Cardiovasc Diabetol 19:19.

Peng S, Wang C, Ma J, Jiang K, Jiang Y, Gu X, Sun C (2018) Achyranthes bidentata polypeptide protects dopaminergic neurons from apoptosis in Parkinson's disease models both in vitro and in vivo. Br J Pharmacol 175:631-643.

Perez-Lloret S, Otero-Losada M, Toblli JE, Capani F (2017) Renin-angiotensin system as a potential target for new therapeutic approaches in Parkinson's disease. Expert Opin Investig Drugs 26:1163-1173.

Rabie MA, Abd El Fattah MA, Nassar NN, El-Abhar HS, Abdallah DM (2018) Angiotensin 1-7 ameliorates 6-hydroxydopamine lesions in hemiparkinsonian rats through activation of MAS receptor/PI3K/Akt/BDNF pathway and inhibition of angiotensin II type-1 receptor/NF-κB axis. Biochem Pharmacol 151:126-134.

Rocha NP, Scalzo PL, Barbosa IG, Campos-Carli SM, Tavares LD, Souza MS, Christo PP, Reis HJ, Simões ESAC, Teixeira AL (2016) Peripheral levels of angiotensins are associated with depressive symptoms in Parkinson's disease. J Neurol Sci 368:235-239.

Scrivo A, Bourdenx M, Pampliega O, Cuervo AM (2018) Selective autophagy as a potential therapeutic target for neurodegenerative disorders. Lancet Neurol 17:802-815.

Shahnawaz M, Mukherjee A, Pritzkow S, Mendez N, Rabadia P, Liu X, Hu B, Schmeichel A, Singer W, Wu G, Tsai AL, Shirani H, Nilsson KPR, Low PA, Soto C (2020) Discriminating α-synuclein strains in Parkinson's disease and multiple system atrophy. Nature 578:273-277.

Stacchiotti A, Corsetti G (2020) Natural compounds and autophagy: allies against neurodegeneration. Front Cell Dev Biol 8:555409.

Tao MX, Xue X, Gao L, Lu JL, Zhou JS, Jiang T, Zhang YD (2018) Involvement of angiotensin-(1-7) in the neuroprotection of captopril against focal cerebral ischemia. Neurosci Lett 687:16-21.

Tong Q, Wu L, Gao Q, Ou Z, Zhu D, Zhang Y (2016) PPARβ/δ agonist provides neuroprotection by suppression of IRE1α-caspase-12-mediated endoplasmic reticulum stress pathway in the rotenone rat model of Parkinson's disease. Mol Neurobiol 53:3822-3831.

Van Den Berge N, Ferreira N, Gram H, Mikkelsen TW, Alstrup AKO, Casadei N, Tsung-Pin P, Riess O, Nyengaard JR, Tamgüney G, Jensen PH, Borghammer P (2019) Evidence for bidirectional and trans-synaptic parasympathetic and sympathetic propagation of alpha-synuclein in rats. Acta Neuropathol 138:535-550.

Wang D, Tran K, Burt DR, Zhong L, Gao GP (2018a) Slow infusion of recombinant adeno-associated viruses into the mouse cerebrospinal fluid space. Hum Gene Ther Methods 29:75-85.

Wang SJ, Wang Q, Ma J, Yu PH, Wang ZM, Wang B (2018b) Effect of moxibustion on mTOR-mediated autophagy in rotenone-induced Parkinson's disease model rats. Neural Regen Res 13:112-118.

Xilouri M, Brekk OR, Stefanis L (2016) Autophagy and alpha-synuclein: relevance to parkinson's disease and related synucleopathies. Mov Disord 31:178-192.

Zhou Y, Li M, Zhu DL, Jiang T, Gao Q, Tang XH, Zhang SG, Lu J, Zhang YD (2018) Neuroprotective effect of angiotensin-(1-7) against rotenone-induced oxidative damage in CATH.a neurons. Toxicol In Vitro 50:373-382.

Zou J, Guo Y, Wei L, Yu F, Yu B, Xu A (2020) Long noncoding RNA POU3F3 and α-synuclein in plasma L1CAM exosomes combined with β-glucocerebrosidase activity: potential predictors of Parkinson's disease. Neurotherapeutics 17:1104-1119.